

Simultaneous Adsorptive Removal of Methylene Blue and Copper Ions from Aqueous Solution by Ferrocene-Modified Cation Exchange Resin

Qian Wang, Dehua Zhang, Senlin Tian, Ping Ning

Faculty of Environmental Science and Engineering, Kunming University of Science and Technology, Yunnan, Kunming 650500, China

Correspondence to: D. Zhang (E-mail: zhangdehua_kmust@sina.com)

ABSTRACT: Resin was modified with ferrocene (Fc) to enhance removal of Methylene Blue (MB) and Cu^{2+} from simulated wastewater. The FTIR, N_2 -BET, and X-ray fluorescence analysis confirmed that Fc was successfully grafted onto the surface of resin. The adsorption capacity of Fc modified cation exchange resin (FMCER) was calculated to be 392.16 mg/g Cu^{2+} and 10.01 mg/g MB. Both processes were spontaneous and exothermic, best described by Langmuir equation. Pseudo-first-order kinetic model satisfied the adsorption of MB, while the intraparticle-diffusion model fitted the kinetics of Cu^{2+} adsorption best. The result revealed a multilayer adsorption of Cu^{2+} on FMCER, and the kinetics maybe controlled by intraparticle diffusion, film diffusion, and competition force. The adsorption of MB and Cu^{2+} on FMCER were physicosorptive, with activation energies of 2.09 and 1.27 kJ/mol. pH 2–7 and 4–5 are optimum for the removal of MB and Cu^{2+} , and pH 4 is optimal for the simultaneous removal of MB and Cu^{2+} . © 2014 Wiley Periodicals, Inc. *J. Appl. Polym. Sci.* **2014**, *131*, 41029.

KEYWORDS: adsorption; kinetics; resins; dyes/pigments

Received 18 January 2014; accepted 15 May 2014

DOI: 10.1002/app.41029

INTRODUCTION

More than 2000 chemicals (dyes and agents) are used in textile industry,¹ and 20% of these are discharged as textile industrial effluents without any pretreatment.² Some inorganic salts (such as copper sulfate) were used in the textile process in order to assist the solid of color and uniform the blooming.³ Thus, metal ions exist simultaneous with dyes in effluents discharged.

Textile wastewater has been considered as a serious environment offender, for its damage on the public's health and the toxicity to biological systems.⁴ Textile wastewaters are usually of high chemical oxygen demand (COD), and toxic, with low light penetration,⁵ which may decrease the photosynthetic efficiency of aquatic plants.⁶

Many efforts have been made in mitigating the negative influences. Conventional methods including photolysis,⁷ ozonation,⁸ membrane extraction,^{9,10} filtration,^{11,12} and biological process¹³ are used in the treatment of dyeing wastewaters. The high cost, requirement of long time, and the complex processes have limited the wide application of the technologies mentioned above. Adsorption is considered a promising technology in treatment of wastewaters containing low concentration of heavy metals or dyes. Advantages of adsorption are simplistic, ease of operation, and non-introduction of extra energies and toxicities. Materials

such as zeolites,¹⁴ starch graft copolymers,¹⁵ activated carbon,¹⁶ hydrous oxides,¹⁷ saw dust,¹⁸ etc., have already been used successfully in wastewater treatment as adsorbents. Magnetic chitosan composites¹⁹ and grafted chitosan²⁰ were reported of high efficiencies for the adsorptive removal of dyes and metal ions from simulated water, but with drawbacks of complex synthesis process and limited range of pH window.

Resin has already been focused on since several years ago. Especially, it was widely used in environmental pollution remediation of both organics and inorganics.^{21–23} It has been successfully used in the adsorptive removal of precious metals^{24–26} (Au, Ag, Cu, Cr, etc.) and dyes^{5,27} (basic yellow 87, reactive blue). But investigations on treatment of dyes and metal ions from simulated wastewaters were not enough, which might give more effective guidance to treatment of real wastewaters discharged from industries. Vidhyadevi et al.,²⁸ proposed the use of poly azomethineamide resin as adsorbent for the removal of Cd^{2+} and Methyl Red simultaneously. But the synthesis process of the adsorbent is complex.

This study attempts to prepare a low-cost and high-effective adsorbent for the simultaneous removal of Cu^{2+} and MB in aqueous solution. Cation exchange resin was chosen for its wide application and cost efficiency, but with drawbacks of the limited range of pH and low adsorption capacity. Ferrocene (Fc) is

Table I. SQX Calculated Results of Untreated Resin and FMCER (%)

Component	Untreated Resin	FMCER
C	97.5416	96.0021
S	1.2748	2.7353
Na	0.3668	0.4862
Fe	0.0037	0.0580
Others	0.8131	0.7184

electron-rich, and it can lose an e^- to form Fc^+ , and be regenerated by obtaining an e^- , which characteristic may allow it alleviate the repulsion in the adsorption process. Thus, Fc was chosen to modify the cation exchange resin in this study, in order to enlarge the pH window for the adsorption onto resin. Comparison of the structure and the physicochemical characteristics of the untreated resin and the Fc modified cation exchange resin (FMCER) were done through Fourier transform infrared spectroscopy (FTIR), Brunauer-Emmett-Teller isotherm (BET), and X-ray fluorescence (XRF) analysis. Influences of parameters such as initial solution pH, reaction temperature, initial concentration, and the dose of adsorbent on Cu^{2+} removal were investigated. The adsorption isotherms, kinetics, and thermodynamics for the removal of MB and Cu^{2+} were examined.

EXPERIMENTAL

Reagents

Cation exchange resin (001×7) was obtained from Daomao Chemical Reagent Plant; Alcohol, Methylene Blue, $CuSO_4$, and NaOH were purchased from Sinopharm Chemical Reagent Co. Ltd., Shanghai, China; Fc was obtained from Jingchun Chemical Reagent Co. Ltd., Shanghai, China; H_2SO_4 was obtained from Chuandong Chemical Reagent Co. Ltd., Chongqing, China. All chemicals used in this study are analytical grade and all solutions used are prepared daily using deionized water made from Millipore system with a resistivity of 18.25 MΩ cm.

Preparation of the Fc Modified Cation Exchange Resin

The modification process was performed in a 3-L reactor. Firstly, 100 g of the cation exchange resin (001×7) was dispersed in 250 mL mixed acids ($HCl : HNO_3 = 1 : 1$) and kept intense shaking for about 2 h to remove impurities. After that, the resin was washed with deionized water repeatedly until neutral and dried at room temperature after being filtrated out. In the synthesis step, 1 L of alcohol was used as solvent, 300 g of resin was mixed with 100 g of Fc, stirred at the speed of 150 rpm, at 303 K, and the reaction time was 6 h. The product was filtered to be separated and the solid phase was washed with alcohol to remove the excessive Fc. The solid obtained was dried at room temperature for 24 h, and then dried at 353 K for 3 h. The product was used as adsorbent and stored in a sealed bottle.

The structure of the materials was investigated by means of N_2 -BET analysis performed on a Micromeritics TriStar II unit. Pore distributions and pore volumes were calculated using the adsorption branch of the N_2 isotherms based on BET equation. Elemental analysis of the two adsorbents was obtained from XRF analysis, and the analysis was performed on a Rigaku ZSX100e instrument. Characterization of Fc loaded on the

cation exchange resin was performed by FTIR using a Varian 600-IR spectrometer.

Batch Experiments

All experiments were carried out in batch using flasks (250 mL) with resin/liquid ratio of 1 g/L. The whole process was kept stirred at the rate of 275 rpm at 303 K. The mixture of MB and Cu^{2+} was prepared by dissolving given amounts of MB and $CuSO_4 \cdot 5H_2O$ in deionized water and the solution was freshly prepared daily.

To determine the optimal time required for MB and Cu^{2+} removal by FMCER, 0.1 g adsorbent was added into 100 mL of 640 mg/L $CuSO_4 \cdot 5H_2O$ and 10 mg/L MB solution and stirred for 10–420 min at pH 4.

The effect of pH on adsorption was investigated at initial Cu^{2+} concentration of 640 mg/L and MB 10 mg/L performed with solution pH varied from 2 to 7 at 303 K. The initial solution pH was adjusted using 1 mol/L NaOH and H_2SO_4 solution.

The influence of various dose of adsorbent (0–2.0 g/L) on the adsorptive removal of MB and $CuSO_4 \cdot 5H_2O$ was investigated at 303 K.

The adsorption isotherms were studied at 293, 303, and 313 K. A 100 mL 640 mg/L $CuSO_4$ and 10 mg/L MB mixture was equilibrated with 0.1 g FMCER for 420 min. Samples obtained at time intervals were filtered through a 0.45- μ m filter membrane after adsorption.

The residual Cu^{2+} in solution was determined on an atomic absorption spectrophotometer (Shimadzu AA 6300C); residual MB in solution was detected using a UV-vis spectrometer (Shimadzu 2450).

The adsorptive removal efficiency (%) of adsorbate on FMCER and the amount of adsorbate adsorbed (q_e) were calculated respectively, from the following equations:

$$\eta = \frac{C_0 - C_e}{C_0} \times 100\% \quad (1)$$

$$q_e = \frac{V(C_0 - C_e)}{m} \quad (2)$$

where C_0 (mg/L) is the initial concentration of Cu^{2+} /MB, C_e (mg/L) is the concentration of Cu^{2+} /MB at equilibrium, V (L) is the volume of solution, and W (g) is the mass of adsorbent. Adsorption kinetics was also investigated, and the quantity of Cu^{2+} /MB (q_t , mg/g) adsorbed at time t was calculated using the following equation:

$$q_t = \frac{V(C_0 - C_t)}{m} \quad (3)$$

where C_t (mg/L) is the concentration of Cu^{2+} /MB at time t .

RESULTS AND DISCUSSION

Characterization of FMCER

The loading of Fc on cation exchange resin was determined by XRF and the results are shown in Table I. The increase of Fe indicated that Fc was successfully modified onto cation exchange resin. The calculated increased amount of Fe was 0.05%, meaning 0.19% (wt/wt) of Fc in FMCER.

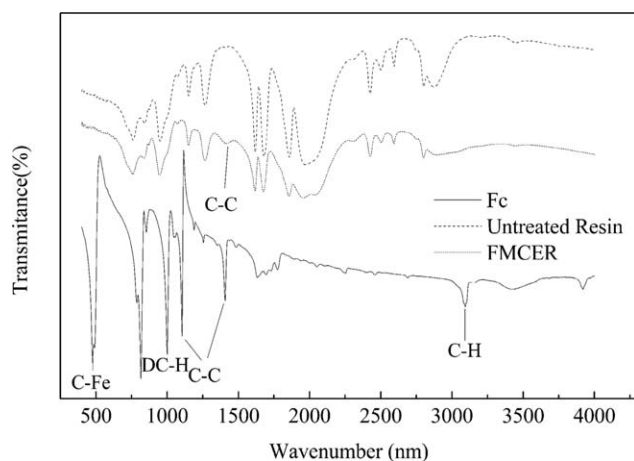


Figure 1. FTIR analysis of FMCER.

The FTIR spectra of Fc, untreated resin, and FMCER in the range of 4000–400 cm^{-1} are shown in Figure 1. As shown in Figure 1, the peaks at 485.98 cm^{-1} , 1407.83 cm^{-1} and 1105.33 cm^{-1} , 998.96 cm^{-1} , 3091.38 cm^{-1} can be ascribed to C–Fe band, C–C band in cyclopentane, DC–H and C–H band in the spectra of Fc, respectively. All peaks of the untreated resin can be observed in the spectra of FMCER, indicating that the framework of resin was kept well after the modification. No absorbance of 485.98 cm^{-1} and 3091.38 cm^{-1} could be found in the spectra of FMCER, this result indicated that C–Fe band in Fc molecular broke, but the absorbance at 1407.83 cm^{-1} appeared after the modification of resin with Fc. All the results mentioned above indicated that cation exchange resin has been chemical modified by Fc successfully. C–Fe in Fc broke and C in cyclopentane connected to the surface of cation exchange resin.

As shown in Figure 2 and Table II, the surface characterization of FMCER shows that its micropore surface area (S_{MP}) is measured to be 1.69 m^2/g , and the pore diameters mainly distributed at 2.08, 2.76 and 4.79 and 6.34 nm, while the S_{MP} of untreated resin is measured to be 2.17 m^2/g and the pore diameters are 1.89, 2.39, 3.69, and 5.38 nm. Both the S_{MP} and pore diameters of FMCER are both decreased from the untreated resin in the

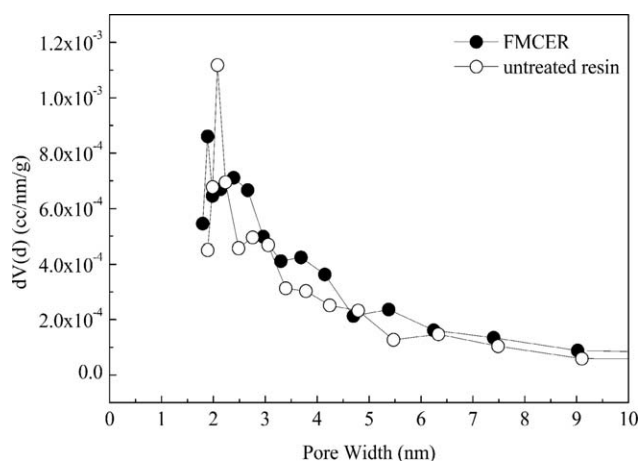


Figure 2. Pore size distributions of FMCER and untreated resin.

Table II. Untreated Resin and FMCER Characterization Data

	Untreated resin	FMCER
S_{MP} (m^2/g)	2.17	1.69
Pore width (nm)	2.08	1.89
	2.76	2.39
	4.76	3.69
	6.34	5.38

modification process. The reason maybe that Fc was connected to the external surface and the micropore surface of the resin. Thus, the diameters of the pores of resin decreased after the modification and the S_{MP} decreased accordingly.

Influences of Important Factors on the Simultaneous Adsorptive Removal of MB and Cu^{2+} onto FMCER

Influence of Reaction Time on Adsorption. The equilibrium time is assisted to be found out in the effect of contact time on the adsorption of MB and Cu^{2+} onto FMCER, and the correlations between the amount of MB/ Cu^{2+} adsorbed onto the fixed amount of adsorbent and the reaction time can also be ascertained. The effect of contact time (0–420 min) on the adsorption capacity of MB/ Cu^{2+} in simulated wastewater and Cu^{2+} aqueous solution were studied and the results are given in Figure 3. The results indicated that the removal efficiency and the adsorptive removal of Cu^{2+} and MB increased as the reaction progressed, since at the beginning of the reaction, the initial concentrations provide an important driving force to overcome the mass transfer resistance of MB and Cu^{2+} between the liquid phase and the solid phase.²⁹ With the passage of time the initial concentration decreases and consequently the driving force, Cu^{2+} and MB were adsorbed onto FMCER through cation exchange on surface of the resin. Points need to be emphasized are: firstly, the adsorptive removal of Cu^{2+} from simulated wastewater was much slower from simulated wastewater than that from Cu^{2+} aqueous solution. The adsorption capacity was also decreased with the presence of MB, which was attributed to the competition of MB. Secondly, the adsorptive removal of MB is much faster after 2.5 h than in the beginning of the reaction. The reason maybe that the diameter of Cu^{2+} is much smaller than that of MB molecular, and the bulk of MB in solution exist as MB^+ , thus, the competition between MB^+ and Cu^{2+} resisted the approaching of MB^+ to FMCER; on the other hand, the transformation $\text{Fc} \leftrightarrow \text{Fc}^+$ occurred on the surface of FMCER and the ion leached into aqueous surrounding FMCER to decrease the repulsion and the competition. The adsorption of MB reached equilibrium at 7 h, while the adsorptive removal of Cu^{2+} attained the equilibrium at about 6 h. Thus, in this study, 7 h was chosen as the contact time to reach equilibrium and used in the following studies.

Influence of Solution pH on Adsorption. Initial solution pH has been reported as an important parameter that influences the adsorption of metal ions and dye molecules.³⁰ In this study, the adsorption of MB and Cu^{2+} were both discussed at the range of initial solution pH 2–7, because the Cu^{2+} precipitated under alkaline conditions. Adsorption processes with a fixed 100 mL, 10 mg/L MB, and 640 mg/L CuSO_4 aqueous solution

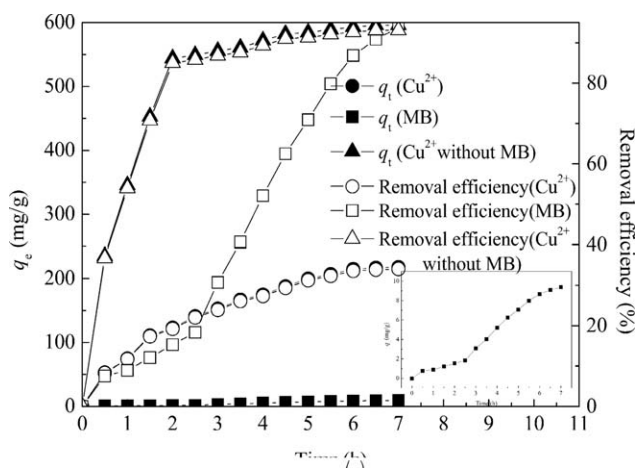


Figure 3. Influence of contact time on the adsorption of MB and Cu^{2+} on FMCER.

at various pH values were designed to examine the effect of pH, and the results are shown in Figure 4. The adsorption capacities of MB and Cu^{2+} onto FMCER both increased as the initial solution pH increased from 2 to 4 to reach a plateau and the maximum adsorption capacities were obtained as 247.13 mg/g and 9.18 mg/g for Cu^{2+} and MB, respectively, at pH 4, which means 38.59% removal of Cu^{2+} and 91.84% removal of MB from aqueous solution. High removal efficiencies for both Cu^{2+} and MB were shown at pH 4 and 5. The removal efficiencies of MB and Cu^{2+} at pH = 5 were detected to be 91.84% and 38.28% respectively, and the adsorption capacities were calculated to be 9.18 and 245.06 mg/g. The uptake of MB and Cu^{2+} decreased as the solution pH further increased, and the removal efficiencies of MB and Cu^{2+} at pH 7 were determined to be 87.63% and 27.03%, and the adsorption capacities were calculated to be 8.76 and 173.01 mg/g, accordingly. The reasons maybe that the properties of adsorbent (surface charge) and adsorbate (degree of ionization and dissociation of functional groups) varied under different operating conditions,³¹ and the suppression of the electrostatic repulsion impede the approaching of the adsorbates to FMCER; the Fc loaded on the surface of resin can easily donate or accept an e^- , which helped buffering the electrostatic repulsion and strengthening the attraction. Thus, initial solution pH has influenced the performance of FMCER a lot, and pH 4 and 5 were determined to be the optimum pH window for the adsorption of MB and Cu^{2+} .

Influence of Adsorbent Dose on Adsorption. Various concentrations of FMCER (0–2.0 g/L) combined with a fixed 100 mL, 10 mg/L MB and 640 mg/L CuSO_4 at the optimum pH were investigated. The adsorption capacities and removal efficiencies at the equilibrium of both Cu^{2+} and MB are shown in Figure 5. The results revealed that both the adsorption capacities and the removal efficiencies increased as the dose of adsorbent increased in the limit ranges of 0–0.25 g/L for MB and 0–1.0 g/L for Cu^{2+} . The maximum q_e of 247.13 mg/g for Cu^{2+} and 29.58 mg/g for MB were reached with the adsorbent dose of 1.0 g/L and 0.25 g/L, respectively. The adsorption capacities of Cu^{2+} as well as MB showed inverse relationship to adsorbent dose in further increase. This phenomenon is favored in studies for making the best use

of adsorbent. The MB removal efficiency increased and reached a plateau at about 0.5 g/L, while the removal efficiency of Cu^{2+} increased as the dose of adsorbent increased. As the removal efficiency of MB increased from 73.96% to 96.39%, the adsorption capacity of Cu^{2+} decreased from 29.58 to 4.82 mg/g, the removal efficiency of Cu^{2+} increased from 38.59% to 50.16% whereas the adsorption capacity decreased from 247.13 to 160.5 mg/g. The reason is that more adsorbent added enabled more available surface area and binding sites for MB and Cu^{2+} in solution.^{32–34} About 1 g/L FMCER was chosen as the optimal condition for the treatment of MB and Cu^{2+} in simultaneous wastewater, for the highest adsorption capacity of Cu^{2+} . Under this condition, most MB in solution can be removed (the removal efficiency was 96.39%). And the FMCER can be withdrawn and further used in the treatment of MB in a new cycle, theoretically.

Adsorption Isotherms

The adsorption isotherms of MB and Cu^{2+} on FMCER at 293, 303, and 313 K were discussed and the results are shown in Figure 6(a,b). The adsorption capacities of MB and Cu^{2+} onto FMCER increased as the initial concentrations of MB and Cu^{2+} increased. Adsorption capacities of MB and Cu^{2+} onto FMCER decreased as temperature increased from 293 to 313 K, indicating that the removal of MB and Cu^{2+} from aqueous by FMCER is an exothermic process. The adsorption capacities of MB and Cu^{2+} according to their initial concentrations of 10 mg/L and 640 mg/L turned out to be 8.23 mg/g and 218.03 mg/g at 303 K.

The experimental data were analyzed following the isotherm models of Langmuir, Freundlich, and Dubinin–Radushkevich.

Langmuir isotherm assumes monolayer adsorption and supposes a finite number of homogeneous adsorption sites,³⁵ and the Langmuir model is described by eq. (4):

$$q_e = \frac{Q_{\max} b C_e}{1 + b C_e} \quad (4)$$

And the linear form of Langmuir model is described by eq. (5):

$$\frac{C_e}{q_e} = \frac{1}{Q_{\max} b} + \frac{C_e}{Q_{\max}} \quad (5)$$

where q_e is the equilibrium adsorptive capacity (mg/g), C_e is the equilibrium concentration (mg/L), Q_{\max} (mg/g) and b (L/mg)

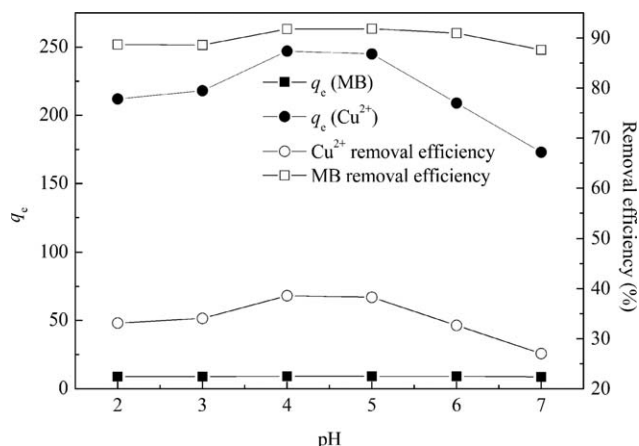


Figure 4. Influence of initial solution pH on the adsorption of MB and Cu^{2+} on FMCER.

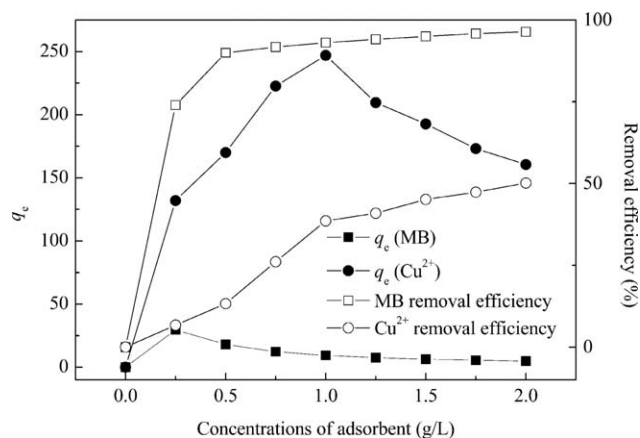


Figure 5. Influence of the dose of adsorbent on the adsorption of MB and Cu²⁺ on FMCER.

are constants related to the maximum adsorption capacity and the energy of the adsorption, respectively.

The separation factor R_L of the Langmuir isotherm which indicates whether the adsorption process is favorable ($0 < R_L < 1$), unfavorable ($R_L > 1$), or linear ($R_L = 1$) can be calculated from eq. (6)³⁶:

$$R_L = \frac{1}{1 + bC_0} \quad (6)$$

The calculated R_L values at different initial concentrations of MB are listed in Table III.

The Freundlich isotherm is an empirical equation assuming that the adsorption process takes place on heterogeneous surfaces and adsorption capacity is related to the concentration of dye at equilibrium. And the Freundlich isotherm model is usually used to satisfy adsorption processes with low concentrations of adsorbate.³⁵ The Freundlich isotherm model is described by eq. (7):

$$q_e = K_F C_e^{\frac{1}{n}} \quad (7)$$

And the linear form of Freundlich model is described by eq. (8):

$$\ln q_e = \ln K_F + \frac{1}{n} \ln C_e \quad (8)$$

where q_e is the equilibrium adsorptive capacity (mg/g), C_e is the equilibrium concentration (mg/L), K_F and n are Freundlich constants that relate the adsorption capacity and the intensity of adsorption, respectively, and can be calculated from Figure 7(b) and the results are shown in Table III.

Dubinin–Radushkevich isotherm model which is based on the Polanyi's adsorption theory is in agreement with adsorption isotherms of microporous adsorbents.²⁹ The Dubinin–Radushkevich isotherm model is described by eq. (9):

$$\ln q_e = \ln q_m - \beta \zeta^2 \quad (9)$$

where q_e is the equilibrium adsorptive capacity (mg/g), q_m is the maximum adsorption capacity (mol/g), and ε is the Polanyi potential given in eq. (10)³⁵:

$$\varepsilon = R \cdot T \ln \left(1 + \frac{1}{C_e} \right) \quad (10)$$

q_m and β can be obtained from Figure 7(c) and listed in Table III.

The results indicated that the Langmuir model was able to properly describe the isotherm of both Cu²⁺ and MB adsorption onto FMCER (correlations coefficient > 0.990). The adsorption capacities of Cu²⁺ and MB were calculated to be 392.16 mg/g and 10.01 mg/g at equilibrium. The Freundlich model also fit the adsorption of Cu²⁺ and MB onto FMCER consistently with correlations coefficient > 0.97. Dubinin–Radushkevich model was also used in this study for the fitting, but the results indicated that the $\ln q_e$ of both Cu²⁺ and MB showed non-linear fit to ε^2 (correlations coefficient < 0.5). R^2 for the linear fit of Cu²⁺ to Langmuir and Freundlich equations are 0.999 and 0.974, respectively. This result indicated that the Langmuir and Freundlich equations both fitted the adsorption of Cu²⁺ well. On comparing the adsorption capacities calculated, Langmuir model is considered to fit the adsorption of MB and fit Cu²⁺ better than Freundlich equation and

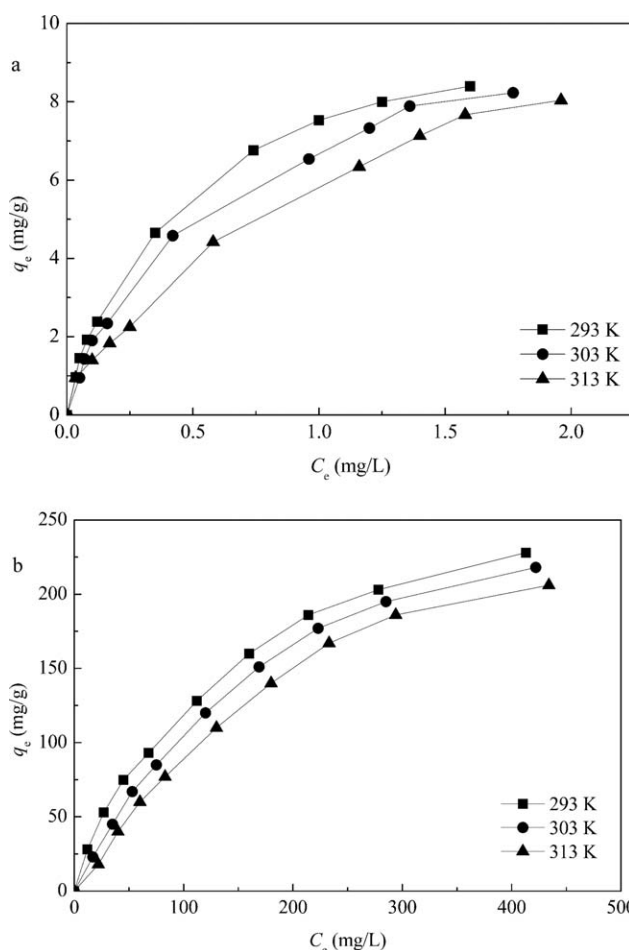


Figure 6. Adsorption isotherm of (a) MB; (b) Cu²⁺ onto FMCER, conditions are: pH = 4, 1.0 g/L FMCER, with the initial MB concentration varied from 0 mg/L to 10 mg/L and the initial Cu²⁺ concentration from 0 mg/L to 640 mg/L.

Table III. Langmuir, Freundlich, and Dubinin–Radushkevich Model Parameters for Adsorption of MB and Cu²⁺ on FMCER

	Langmuir model				Freundlich model			Dubinin–Radushkevich		
	q_e (mg/g)	b	R^2	R_L	n_F	K_F	R^2	Q_m (mol/g)	β (mol ² /kJ ²)	R^2
Cu ²⁺	392.157	0.0037	0.999	0.2976	1.4084	3.6369	0.974	195	-3.427×10^{-6}	0.964
MB	10.009	2.1694	0.990	0.0441	1.7060	6.6212	0.983	4.7998	-0.937×10^{-2}	0.498

monolayer and multilayer adsorption of Cu²⁺ happened simultaneously.

The separation factor R_L of MB and Cu²⁺ adsorption were calculated to be 0.0441 and 0.2976, respectively, which indicated that the adsorption of MB and Cu²⁺ are favorable. On the other hand, the value n of the adsorption of Cu²⁺ onto FMCER is greater than 1 ($n = 1.4084$), which also indicates that the adsorption of Cu²⁺ exhibits a favorable shape and the value $1/n$ reveal a multilayer adsorption of Cu²⁺ onto the active sites on the surface of FMCER.^{37–39}

Adsorption Kinetics

To study the adsorption mechanism well, the pseudo-first order, pseudo-second order, and Weber–Morris models were fitted to experimental data obtained in MB and Cu²⁺ adsorption in order to study the kinetics of the process. The linearized pseudo-first order model represented by Lagergren assumes that the rate of change of solute uptake with time is directly proportional to the difference in saturation concentration and the amount of solid uptake with time,⁴⁰ and the equation is described in the following equation:

$$\ln(q_e - q_t) = \ln q_e - k_1 t \quad (11)$$

where q_e and q_t (mg/g) are the adsorptive uptakes at equilibrium and time t , respectively. k_1 (1/h) is the rate constant of the first-order adsorption. The model parameters q_e and k_1 can be obtained from the intercept and slope of the linear of the plots of $\ln(q_e - q_t)$ vs. t [Figure 8(a)].

The linearized-pseudo-second order model proposed by Ho⁴¹ illustrates the velocity dependence on the capacity of adsorption in the solid phase but no dependence on the concentration of the adsorbed substance is described in the following equation:

$$\frac{t}{q_t} = \frac{1}{k_2 \cdot q_e^2} + \frac{t}{q_e} \quad (12)$$

where k_2 (g/mg·h) is the rate constant of the second-order adsorption. k_2 and q_e can be calculated from the intercept and slope of the linear of the plots of t/q_t vs. t [Figure 8(b)].

The estimated parameters q_e , k_1 , k_2 , R^2 are listed in Table IV.

The adsorption kinetics of Cu²⁺ and MB are presented in Figure 8(a,b). The kinetic data of MB adsorption were better fitted by the pseudo-first order model ($R^2 = 0.848$) than pseudo-second order ($R^2 = 0.163$) and intraparticle diffusion models ($C < 0$). The adsorption of Cu²⁺ followed both the pseudo-first order and pseudo-second order kinetics, especially the pseudo-second order model for the consistent to the experimental data.

It's the difference of the adsorption capacities at equilibrium and any time t that drives the adsorption of the adsorbate onto

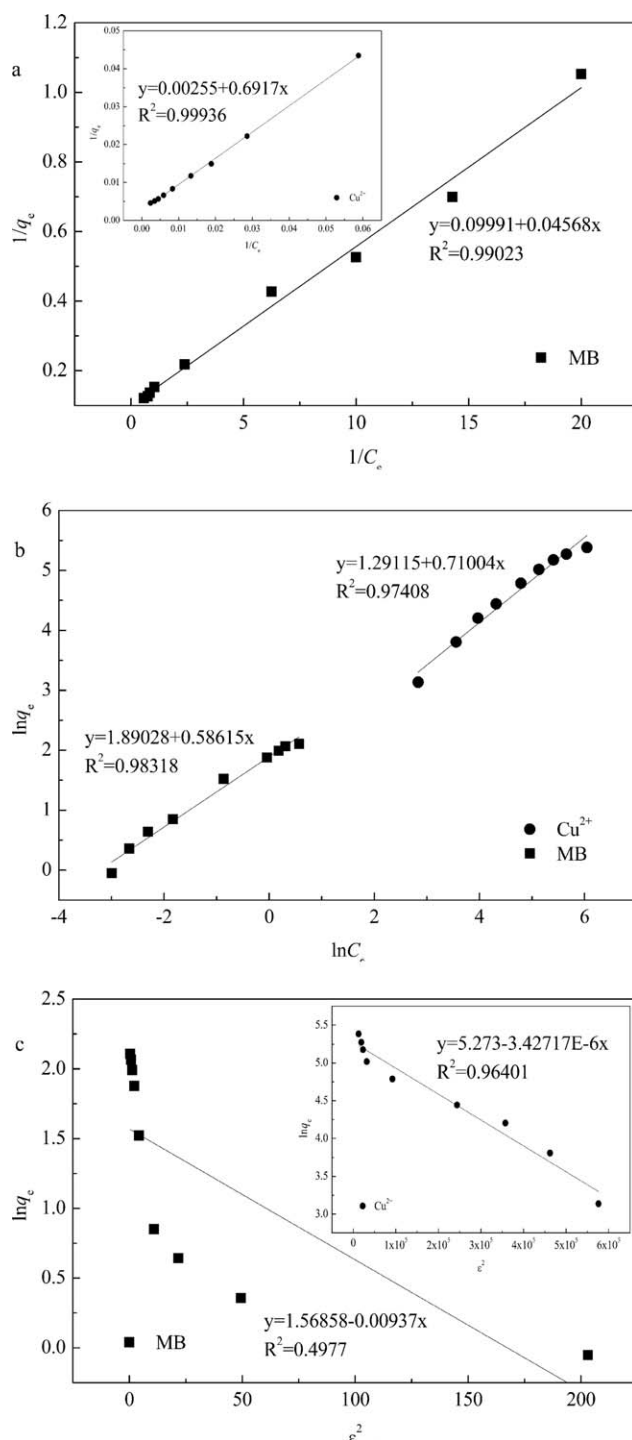


Figure 7. (a) Langmuir; (b) Freundlich; (c) Dubinin–Radushkevich adsorption isotherms fit for MB and Cu²⁺ onto FMCER.

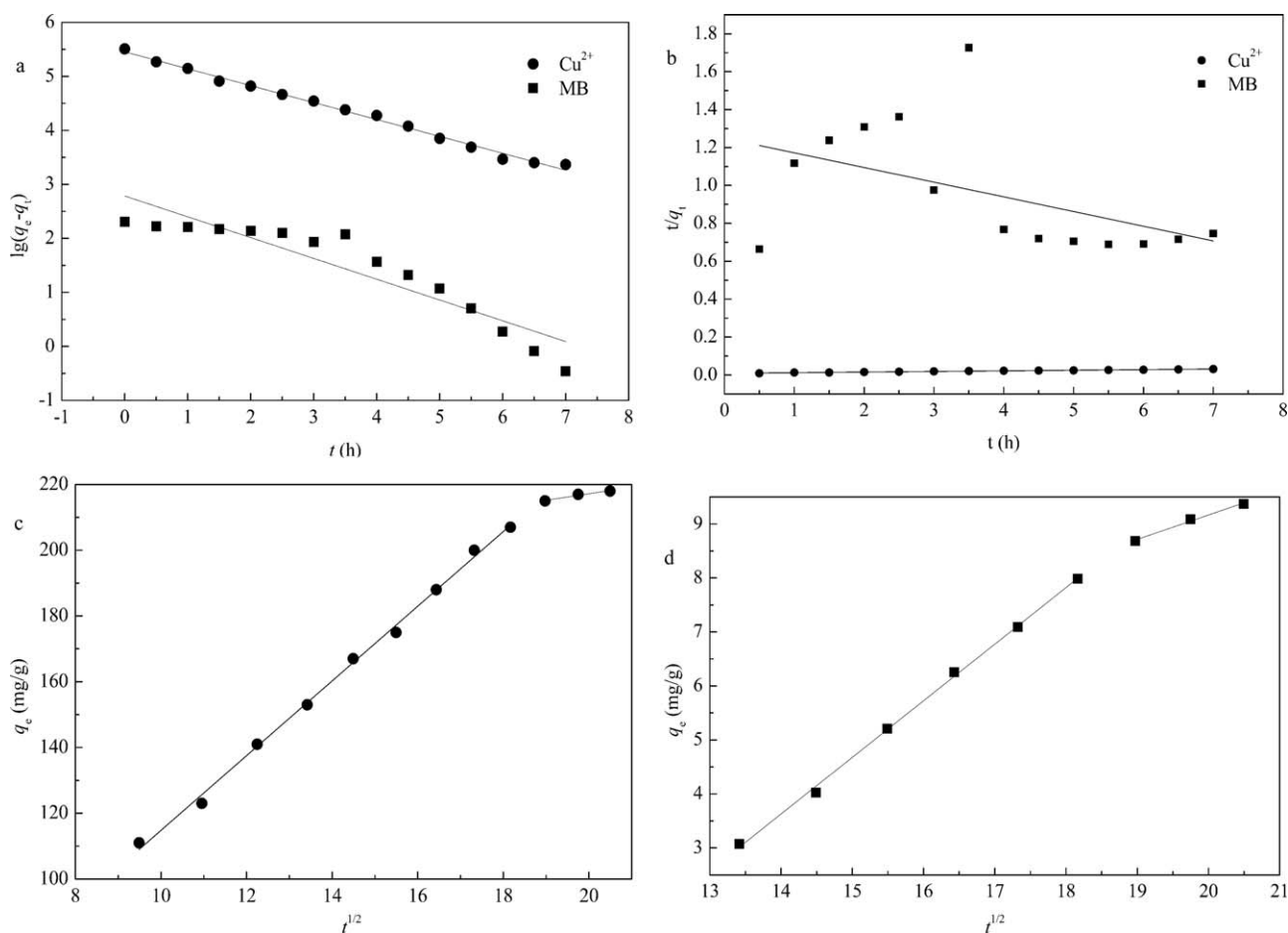


Figure 8. Kinetic plots for the adsorption of MB and Cu^{2+} on FMCER: (a) Pseudo-first order plot; (b) pseudo-second order plot for the adsorption of MB and Cu^{2+} and Weber–Morris kinetic model for the adsorption of (c) Cu^{2+} , and (d) MB on FMCER

adsorbents, and the adsorption capacity is in correlation to the amount of active sites on adsorbent surface.⁴² The pseudo-second order model fitted the adsorption process of Cu^{2+} well: (1) Cu^{2+} in solution diffuse from liquid phase to liquid–solid interface (film diffusion); (2) adsorbate further moved to solid surface and diffuse into particle pores (intraparticle diffusion); (3) adsorption of Cu^{2+} onto the active site in inner and outer surface of FMCER.

Commonly, the rate of adsorption may be controlled by intraparticle diffusion and film diffusion. Herein, the Weber–Morris model was chosen to fit the kinetic adsorption data of Cu^{2+} in order to reveal the contributions of the surface and the intraparticle diffusion to the kinetic process. The Weber–Morris equation is described in the following equation:

$$q_t = k_{id} t^{1/2} + C \quad (13)$$

where C (mg/g) is the boundary layer thickness; k_{id} ($\text{mg/g}\cdot\text{min}^{1/2}$) is the intraparticle diffusion rate constant. The results are shown in Figure 8(c,d), and the parameters are also listed in Table IV.

The kinetics of Cu^{2+} adsorption fit the pseudo-second order of Weber–Morris well ($R^2 = 0.995$), according to the results of fitting experimental data presented in Table IV. The correlation coefficient R^2 of MB adsorption based on pseudo-first order model was much higher than that based on pseudo-second order model. Although the correlation coefficient R^2 of MB adsorption calculated from fitting to the pseudo-first order of Weber–Morris model is 0.998, the boundary layer thickness cannot be obtained. The pseudo-second order of Weber–Morris

Table IV. Kinetic Parameters for MB and Cu^{2+} Adsorption Using FMCER

Kinetic model	Pseudo-first order			Pseudo-second order			Intraparticle diffusion model		
	k_1 (h^{-1})	q_e (mg/g)	R^2	k_2 (g/mg h)	q_e (mg/g)	R^2	K_{id}	C	R^2
Cu^{2+}	0.313	233.7939	0.9931	0.32×10^{-2}	311.527	0.9896	11.3618	1.1794	0.9946
MB	0.385	16.1848	0.8485	4.44×10^{-5}	-134.228	0.1628	1.0482	/	0.9983

Table V. Thermodynamic Data for the Adsorption of MB and Cu²⁺ onto FMCER

Adsorbate	ΔG° (kJ/mol)			ΔH° (kJ/mol-K)	ΔS° (kJ/mol)
	293 K	303 K	313 K		
Cu ²⁺	-1344.2	-1300.73	-1234.59	-5746.6543	-9397.1351
MB	-12782.9	-11707.7	-10669.5	-24.5191	-18.2761

model is most suitable in describing the adsorption kinetic of Cu²⁺, while the pseudo-first order model describes the adsorption of MB better. For Cu²⁺ adsorption, the intraparticle diffusion is an important rate-limiting step, but not the sole, for the $q_t \sim t^{1/2}$ plot does not go through the origin. The kinetics may be controlled by intraparticle diffusion, film diffusion, and the competition force simultaneously. The control of adsorption rate might be possible with a better control of external mass transfer and intraparticle diffusion parameters such as stirring rate and temperature.⁴³

Adsorption Thermodynamics

In order to identify the inherent energetic changes which is associated with the adsorption process, thermodynamic properties and the influence of reaction temperature on the adsorption removal of MB and Cu²⁺ were investigated at 293, 303, and 313 K. Thermodynamic parameters such as change in standard free energy (ΔG°), enthalpy change (ΔH°), and entropy changes (ΔS°) can be determined using eqs. (14) and (15), thermodynamic data can be calculated from the Langmuir equations. The Langmuir constant K_L is related to the enthalpy of adsorption.

$$-\Delta G_{\text{ads}}^\circ = RT \ln(K_L) \quad (14)$$

$$\Delta G^\circ = \Delta H^\circ - T\Delta S^\circ \quad (15)$$

R (8.314 J/mol K) is the gas constant, T (K) is the absolute temperature, and K_L (L/mg) is the standard thermodynamic equilibrium constant defined by Q_e/C_e . The values ΔH° and ΔS° can be calculated from the slope and intercept of Vant's Hoff plots of $\ln K_L$ vs. T^{-1} . The results of ΔG° , ΔH° , and ΔS° are listed in Table V.

The negative ΔG° values at various temperatures indicated the spontaneous nature of the adsorption of MB and Cu²⁺ on to FMCER, revealing an increased randomness at the solid solution interface during the fixation of the dye on the active sites of FMCER. The negative value of ΔH° identified both the adsorption of MB and Cu²⁺ as exothermic processes, indicating that the adsorption capacities are increased as the temperature decreased.^{44–46} Also, the negative value of ΔS° suggests that the

Table VI. Activation Energies Calculated of the Adsorption of MB and Cu²⁺ on FMCER

Adsorbate	MB			Cu ²⁺		
	Parameter	T (K)	k_1 (h ⁻¹)	E_a (kJ/mol)	k_2 (g/mg h)	E_a (kJ/mol)
		293	0.437	2.094	0.0038	1.272
		303	0.385		0.0032	
		313	0.264		0.0028	

randomness decreases the removal of MB and Cu²⁺ on FMCER.⁴⁷

As it has been investigated above, pseudo-first order model fit the adsorption of MB well and the pseudo-second order model was better to fit the Cu²⁺ adsorption experimental data, thus, the rate constant values k_1 and k_2 for the adsorption of MB and Cu²⁺ were used to determine the activation energies, E_a (kJ/mol), for the processes by the Arrhenius equation:

$$\ln k = \frac{-E_a}{RT} + \ln A \quad (16)$$

where A and E_a are Arrhenius factor and the activation energy (kJ/mol), respectively. The rate constants k_1 and k_2 for MB and Cu²⁺ adsorption and the activation energy values obtained at 293, 303, and 313 K are shown in Table VI.

As it can be seen in Table VI, the kinetic rate of the adsorption process decreased as the reaction temperature increased, and the activation energy value determined was 2.094 kJ/mol and 1.272 kJ/mol for adsorption of MB and Cu²⁺, respectively. The activation energy lower than 40 kJ/mol indicates a physical process, while the range of 40–800 kJ/mol means a chemisorption process.⁴⁸ Thus, it can be concluded that the adsorption of MB and Cu²⁺ on FMCER are both physical adsorption process. Actually, both physisorption and chemisorption may occur simultaneously on the surface, a layer of molecules may be physically adsorbed on a top of an underlying chemisorbed layer.⁴⁹

CONCLUSIONS

FMCER was prepared and used in the treatment of wastewater containing MB and Cu²⁺. The BET analysis confirmed that the modification decreased the micropore surface area and pore diameter of cation exchange resin. The FTIR analysis revealed that Fc was grafted to the surface of the resin. Results of the batch experiments designed for the investigation of the adsorption process indicated that the Langmuir isotherm model describes the adsorption of MB well. The kinetic studies show that the adsorption of MB onto FMCER followed pseudo-first order kinetic model, while the adsorption of Cu²⁺ followed Webber–Morris model. The negative value of ΔG° confirmed the spontaneous nature of the adsorption process. The adsorption processes of both MB and Cu²⁺ are physisorptive, and the activation energy (E_a) were calculated to be 2.094 kJ/mol for MB adsorption and 1.272 kJ/mol for Cu²⁺ adsorption.

ACKNOWLEDGMENTS

This work was financially supported by the National Science Foundation of China (20607008; 21077048; 21277064), the Zhejiang Provincial Key Laboratory of Organic Pollution Process and

Control, China, and the Analysis and Testing Foundation of Kunming University of Science and Technology (2010150), Key Project of Chinese Ministry of Education (210202).

REFERENCES

1. Sahoo, M. K.; Sinha, B.; Marbaniang, M.; Naik, D. B. *Desalination* **2011**, *280*, 266.
2. Chakma, S.; Moholkar, V. S. *AIChE J.* **2013**, *59*, 4303.
3. Ogugbue, C. J.; Sawidis, T.; Oranus, N. A. *Ann. Microbiol.* **2012**, *62*, 1141.
4. Daskalaki, V. M.; Timotheatou, E. S.; Katsaounis, A.; Kalderis, D. *Desalination* **2011**, *274*, 200.
5. Wu, X. B.; Hui, K. N.; Hui, K. S.; Lee, S. K.; Zhou, W.; Hwang, D. H.; Cho, Y. R.; Son, Y. G. *Chem. Eng. J.* **2012**, *180*, 91.
6. Hosseneini, S.; Khan, M. A.; Malekbala, M. R.; Cheah, W.; Choong, T. S. Y. *Chem. Eng. J.* **2011**, *171*, 1124.
7. Galindo-Hernández, F.; Gómez, R. J. *Photochem. Photobiol. Chem.* **2010**, *217*, 383.
8. Balcioglu, I. A.; Arslan, I. *Water Sci. Technol.* **2001**, *43*, 221.
9. Yang, S. T.; Chen, S.; Chang, Y. L.; Cao, A. N.; Liu, Y. F.; Wang, H. F. *J. Colloid Interface Sci.* **2011**, *359*, 24.
10. Guo, J.; Kang, L.; Lian, J.; Yang, J.; Yan, B.; Li, Z. C.; Liu, C.; Yue, L. *Biodegradation* **2010**, *21*, 1049.
11. Wu, J. N.; Eiteman, M. A.; Law, S. E. *J. Environ. Eng.* **1998**, *124*, 272.
12. Kim, T. H.; Park, C.; Kim, S. *J. Clean Prod.* **2005**, *13*, 779.
13. Nerud, F.; Baldrian, P.; Eichlerova, I.; Merhautová, V.; Gabriel, J.; Homolka, L. *Biocatal. Biotransform.* **2004**, *22*, 325.
14. Blanchard, G.; Maunay, M.; Martin, G. *Water Res.* **1984**, *18*, 1501.
15. Zhang, L. M.; Chen, D. Q. *Colloid Surf. A* **2002**, *205*, 231.
16. Monser, L.; Adhoum, N. *Sep. Purif. Technol.* **2002**, *26*, 137.
17. Karthikeyan, G.; Elliott, H. A.; Chorover, J. *J. Colloid. Interface Sci.* **1999**, *209*, 72.
18. Ajmal, M.; Hussain Khan, A.; Ahmad, S.; Ahmad, A. *Water Res.* **1998**, *32*, 3085.
19. Reddy, D. H. K.; Lee, S. M. *Adv. Colloid Interface* **2013**, *201–202*, 68.
20. Kyzas, G. Z.; Lazaridis, N. K.; Kostoglou, M. *J. Colloid Interface Sci.* **2013**, *407*, 432.
21. Xie, Y. P.; Jing, K. J.; Lu, Y. H. *Chem. Eng. J.* **2011**, *171*, 1227.
22. Huang, J. H.; Deng, R. J.; Huang, K. L. *Chem. Eng. J.* **2011**, *171*, 951.
23. Monier, M.; Ayad, D. M.; Wei, Y.; Sarhan, A. A. *J. Hazard. Mater.* **2010**, *177*, 962.
24. Fujiwara, K.; Ramesh, A.; Maki, T.; Hasegawa, H.; Ueda, K. *J. Hazard. Mater.* **2007**, *146*, 39.
25. Demirbas, A.; Pehlivan, E.; Gode, F.; Altun, T.; Arslan, G. *J. Colloid Interface Sci.* **2005**, *282*, 20.
26. Gode, F.; Pehlivan, E. *J. Hazard. Mater.* **2003**, *100*, 231.
27. Shuang, C. D.; Yang, F.; Pan, F.; Zhou, Q.; Yang, W. B.; Li, A. M. *Chin. Chem. Lett.* **2011**, *22*, 1091.
28. Vidhyadevi, T.; Murugesan, A.; Kalaivani, S. S.; Premkumar, M. P.; Kumar, V. V.; Ravikumar, L.; Sivanesan, S. *Desalin. Water Treat.*, doi: 10.1080/19443944.2013.801323.
29. Ai, L. H.; Li, M.; Li, L. *J. Chem. Eng. Data* **2011**, *56*, 3475.
30. Rehman, M. S. U.; Munir, M.; Ashfaq, M.; Rashid, N.; Nazar, M. F.; Danish, M.; Han, J. I. *Chem. Eng. J.* **2013**, *228*, 54.
31. DíazGómez-Treviño, A. P.; Martínez-Miranda, V.; Solache-Ríos, M. *Appl. Clay Sci.* **2013**, *80–81*, 219.
32. Safa, Y.; Bhatti, H. N. *Desalination* **2011**, *272*, 313.
33. Javaid, M.; Saleemi, A. R.; Naveed, S.; Zafar, M.; Ramzan, N. *JPICHE* **2011**, *39*, 61.
34. Karaer, H.; Uzun, I. *Desalin. Water Treat.* **2013**, *51*, 2294.
35. Sotelo, J. L.; Ovejero, G.; Rodríguez, A.; Álvarez, S.; García, J. *Chem. Eng. J.* **2013**, *228*, 102.
36. McKay, G. J. *Chem. Technol. Biotechnol.* **1982**, *32*, 759.
37. Nassar, M. M.; El-Deundi, M. S.; Al-Wahbi, A. A. *Desalin. Water Treat.* **2012**, *44*, 340.
38. Auta, M.; Hameed, B. H. *Chem. Eng. J.* **2012**, *198–199*, 219.
39. Auta, M.; Hameed, B. H. *J. Ind. Eng. Chem.* **2013**, *19*, 1153.
40. Lagergren, S. K. *Sven. Vetenskapsakad. Handl.* **1898**, *24*, 1.
41. Ho, Y. S. *Adsorption of Heavy Metals from Waste Streams by Peat*. Ph. D. Thesis, University of Birmingham, Birmingham, UK, **1995**.
42. Alshemeri, A.; Yan, C.; Al-Ani, Y.; Dawood, A. S.; Ibrahim, A.; Zhou, C.; Wang, H. Q. *J. Taiwan Inst. Chem. E* **2014**, *45*, 554.
43. Apiratikul, R.; Pavasant, P. *Bioresour. Technol.* **2008**, *99*, 2766.
44. Gupta, V. K.; Carrott, P. J. M.; Ribeiro Carrott, M. M. L.; Suhas, T. L. *Crit. Rev. Environ. Sci. Technol.* **2009**, *39*, 783.
45. Ho, Y. S.; McKay, G. *Chem. Eng. J.* **1998**, *70*, 115.
46. Gupta, V. K.; Kumar, P. *Anal. Chim. Acta* **1999**, *389*, 205.
47. Manju, G. N.; Raji, C.; Anirudhan, T. S. *Water Res.* **1998**, *32*, 3062.
48. Nollet, H.; Roels, M.; Lutgen, P.; Vander Meeren, P.; Verstraete, W. *Chemosphere* **2003**, *53*, 655.
49. Denizli, A.; Say, R.; Arica, Y. *Sep. Purif. Technol.* **2000**, *21*, 181.